Femtosecond Spectroscopic Investigation of the Carrier Lifetimes in Digenite Quantum Dots and Discrimination of the Electron and Hole Dynamics via Ultrafast Interfacial Electron Transfer†

Yongbing Lou, Xiaobo Chen, Anna C. Samia, and Clemens Burda*

Center for Chemical Dynamics and Nanomaterials Research, Department of Chemistry, Case Western Reserve University, 10900 Euclid Avenue, Cleveland, Ohio 44106

Received: June 8, 2003; In Final Form: September 9, 2003

For the Cu_xS system there exists several known solid phases such as Cu_2S (chalcocite), $Cu_{1.8}S$ (digenite), $Cu_{1.96}S$ (djurleite), and CuS (covellite). All of these phases have been identified as p-type semiconducting materials due to copper vacancies within the lattice, which is responsible for their usefulness as optoelectronic materials. The different Cu_xS phases show reportedly low band gap energies of ≥ 1.2 eV for the bulk, which makes them potentially ideal for application purposes of photoinduced voltaics or catalysis where activation through visible light is desired. In this study, we report on the femtosecond carrier dynamics of digenite copper sulfide quantum dots. Digenite quantum dots were prepared by a single source precursor type process and the optical transitions and dynamic properties of the photoinduced charge carriers in these novel nanomaterials characterized by femtosecond time-resolved spectroscopy. It is found that the larger quantum dots have longer excited-state lifetimes, which implies a strong surface-induced effect on the relaxation dynamics. In addition, the dynamics of the electron was differentiated from that of the hole by employing the technique of rapid (<100 fs) electron trapping at adsorbed organic electron acceptors such as benzoquinone.

Introduction

Nanometer-sized materials are important in the development of next generation electronic and optoelectronic devices due to their small size, size dependent properties and large surface-to-volume ratio, which lead to unique chemical and physical properties different from their bulk counterpart.[1,2] Prototype devices based on nanometer-sized materials, such as light-emitting diodes[3,4] and photovoltaic cells,[5] have already been realized. Their functionality is largely determined by the spectroscopic and optoelectronic properties of the semiconductor quantum dots. Therefore, the spectroscopic investigation of the charge carrier dynamics after laser excitation in semiconductor quantum dots has obtained much attention during recent years.[6] The main aspects of the dynamics in nanometer-sized semiconductors are the lifetimes of carrier cooling and trapping. The dynamics have been well studied in several different types of semiconductor quantum dots, such as CdS,[7−9] CdSe,[10−14] InP,[15−17] SnO.[18] In most cases, carrier trapping occurs within a few picoseconds.

Upon photoexcitation of semiconductor quantum dots, the photogenerated electrons and holes undergo spatial separation.[19] Separated photogenerated carriers can thereby produce a photovoltage and a photocurrent (photovoltaic effect);[20−22] alternatively, the separated carriers can drive electrochemical oxidation and reduction reactions (redox reactions) at the semiconductor surface (photoelectrochemical energy conversion, photocatalyst).[23] Obviously, the dynamics of carrier cooling is an extremely important factor for these practical device applications. The carriers need to be extracted to the surface *before* they cool to the band edges and recombine. In other words, long recombination times are desired for these applications and the ability to slow the overall relaxation rate of the excited carriers would then provide a means to enhanced photovoltage.

In photovoltaics, efficient spatial separation of the electron−hole pair is an important requirement. In a quantum dot-based photovoltaic device, the electron is driven by the internal voltage defined by the barrier height of the junction created between the semiconducting nanomaterials and then recombines with a hole at the anode. Such a photovoltaic effect was recently demonstrated in a cell consisting of self-assembled CdSe nanorods.[24,25] Among the different materials considered for these applications, chalcocite (Cu_2S) has been a candidate of choice coupled to the n-type CdS material for photovoltaic devices.[26] However, cation diffusion problems have been observed in this system. The use of copper-deficient digenite ($Cu_{1.8}S$) quantum dots as the absorber layer could thereby overcome the known problems of diffusion of copper ions into the CdS phase on the heterojunction.

Metal sulfide quantum dots have interesting optical and electrical properties.[27−30] In particular, copper sulfides have the ability to form various stoichiometries, whereby Cu_xS ($x = 1$, 2) quantum dots have been synthesized by utilizing different capping molecules.[31] Furthermore, the ground-state electronic absorption spectra of the Cu_xS quantum dots show three distinct types of Cu_xS formed: a green type assigned to crystalline CuS, and two brown types assigned to crystalline Cu_2S and amorphous Cu_2S.

Novel $C_{1.8}S$ quantum dots have been recently prepared using a single source precursor type method and investigated in the light of its photovoltaic aspects.[32] Here, we present a study of the relaxation dynamics of photoexcited $Cu_{1.8}S$ quantum dots with femtosecond pump−probe spectroscopy. The spectral dynamics in the visible range give us a mechanistic picture about

† Dedicated to Prof. M. A. El-Sayed on the occasion of his 70th birthday.

* Corresponding author. E-mail: burda@cwru.edu.

10.1021/jp035618k CCC: $25.00
Published on Web 10/18/2003

the relaxation pathway of the excited charge carriers in $Cu_{1.8}S$ NPs. In addition, by using electron quenchers to the photoexcited quantum dots, we could assign the observed dynamics to either the electron or the hole. The prospects for photovoltaic application based on copper sulfide quantum dots will also be discussed.

Experimental Section

Synthesis of $Cu_{1.8}S$ Quantum Dots with a Single Source Precursor. $Cu_{1.8}S$ quantum dots were synthesized by using a single source precursor method, which involves the decomposition of the copper(II) dithiocarbamate complex in a high-boiling coordinating solvent, as previously described.[32] To prepare the quantum dots, a solution consisting of 1.5 mmol of $Cu(S_2CNEt_2)_2$ in 11.0 mmol of TOPS was injected at 250 °C into a 10.0 mmol solution of TOPO. All reactions were carried out under an Ar atmosphere. The progress of the reaction was monitored by extracting 0.15 mL aliquots from the reaction flask and quenching in 5 mL of toluene. Aliquots were drawn at time intervals of 1, 2, 5, 10, 20, and 40 min and immediately examined by UV−vis as well as fluorescence spectroscopy. The prepared quantum dots were found to be stable and dispersed as a clear sample in toluene over a period of months. The dried nanocrystal powder was analyzed by X-ray powder diffractometry to confirm the $Cu_{1.8}S$ digenite phase and transmission electron microscopy was used to determine the size and shape of the formed quantum dots.

Instrumentation. The UV−vis absorbance and fluorescence spectra were measured on a Varian Cary 50 and a Varian Eclipse fluorescence spectrophotometer, respectively. The X-ray analysis of the samples was carried out using a Philips PW3710 X-ray powder diffractometer. The femtosecond time-resolved transient absorption measurements were recorded on a laser pump−probe system consisting of an amplified erbium-doped fiber laser, which is frequency doubled to 780 nm and amplified in a regenerative amplifier (Clark MXR CPA 2001). This femtosecond laser produces pulses with 120 fs fwhm duration and 800 μJ output energy per pulse at a repetition rate of 1 kHz. A small portion of the fundamental output pulse train is used to generate white light in a 2 mm sapphire crystal whereas the remaining laser light is used to either frequency double or triple the fundamental to achieve 390 or 260 nm, respectively. To obtain different excitation wavelengths, an optical parametric amplifier (OPA) is employed to facilitate the sum frequency mixing and doubling of the signal or idler. Likewise, the probe wavelength range is extended beyond the white light spectrum by using an OPA, which includes difference frequency mixing techniques for probing in the mid-IR range. The pump−probe experiments are all carried out at ambient temperature. For the femtosecond laser spectroscopy measurements, the excitation beam is modulated by a chopper with a 100 Hz frequency. The probe light is used with reflective optics to avoid white light dispersion. Measurements are conducted with the excitation beam focused to a spot diameter of about 500 μm and the probe beam to 100 μm. The quantum dot solution was placed in a 2 mm path length quartz cuvette and continuously stirred by a cell stirrer to avoid permanent bleaching of the pump−probe volume element in the solution. Labview-assisted data acquisition results in 2-dimensional matrixes (wavelength versus delay time), which are then analyzed by the single-value decomposition method.[33] This enabled global analysis of the spectrum-time matrix before proceeding toward kinetic analysis at single wavelengths.

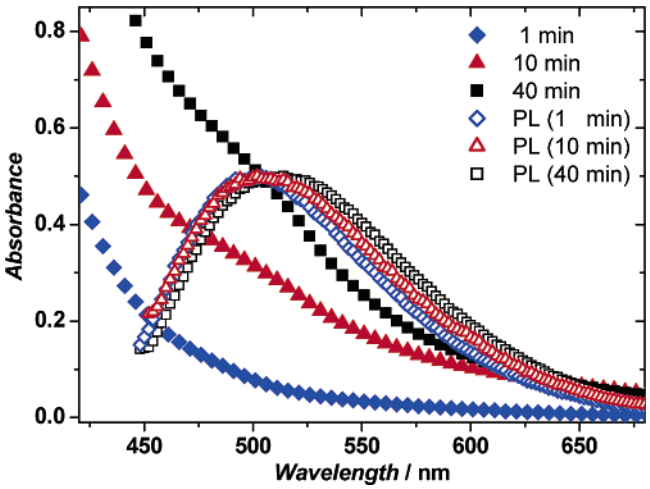

Figure 1. Absorption spectra (filled symbols) of aliquots drawn at 1 (diamonds), 10 (triangles), and 40 (squares) min reaction time during the synthesis of Cu_xS quantum dots. The absorption spectra show shoulders around 480, 495, and 510 nm. The corresponding photoluminescence spectra are shown for the three samples on an arbitrary scale, displaying a decreasing Stokes shift for larger quantum dots.

Results and Discussion

Absorption and Emission Spectra. Shown in Figure 1 are the absorption spectra for three aliquots of the Cu_xS quantum dot mixture (filled symbols) and their corresponding emission spectra (open symbols). For the absorption spectra, the formation of a distinct absorption band at 510 nm is apparent after $\sim^1/_2$ h of precursor pyrolysis. The red shift during the particle growth from 450 to 510 nm is due to the quantum confinement effect typical for low-dimensional semiconductors. The emission spectrum of the Cu_xS quantum dots revealed a bathochromic shift as the quantum dot size increases. The observed changes for the emission maximum are smaller than the changes for the absorption onset. This indicates that the absorption occurs due to excitation into intrinsic electronic states, but the emission occurs from trapping sites. Therefore, the emission spectra do not reflect the changes in quantum dot size as pronounced as the absorption.

The band edge absorption is strongly blue shifted compared to the bulk material (950 nm, 1.1 eV). This is expected due to the spatial confinement or quantum confinement. As growth of the quantum dots occurs, there is a red shift in the absorption and emission wavelength observable. In addition, the Stokes shift (energy difference between the lowest energy absorption and highest energy emission) decreases during the growth of the quantum dots. The trend in Stokes shifts is an indication that the emitting state is composed of deeper trap states for smaller particles and assumes more shallow-trap character as the particle grows.

Powder X-ray Diffraction. The powder X-ray diffraction pattern was measured for the particles formed after 40 min of pyrolysis following our modified single source precursor method. The XRD patterns were fitted to the $Cu_{1.8}S$ (digenite) phase of the Cu_xS family, ruling out other phases that were previously obtained as nanoscaled materials. For example, Zhang et al.[31] have prepared the covelite phase under low-temperature conditions, and Klimov was studying Cu_xS ($x = 1.8-2$) quantum dots in glasses.[34]

Femtosecond Time-Resolved Spectroscopy. *a. Femtosecond Transient Spectra.* Upon femtosecond laser excitation of the $Cu_{1.8}S$ quantum dots, a strong excited-state absorption from 450 to 750 nm, with a maximum around 600 nm, was observed

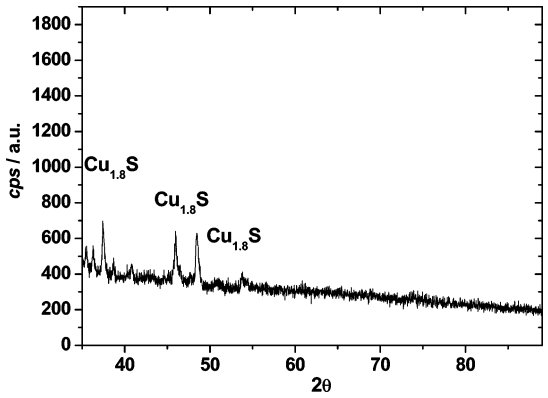

Figure 2. XRD pattern obtained from the sample after the pyrolysis reaction with an equimolar addition of TOPS yielding digenite ($C_{1.8}S$) quantum dots.

(Figure 3). This transient absorption band is bell-shaped and almost symmetric around the 600 nm peak. In addition, a dip was monitored in the spectral range between 450 and 550 nm. Furthermore, the overall peak intensity was excitation power dependent, as illustrated in the inset of Figure 3. Analysis of the intensity of the transient features versus excitation pump power strongly suggests the interpretation of the observed transient absorption as an absorption resulting from the population of trapping sites. The utilized pump power caused multiple excitations but was obviously still in the linear range and no saturation occurred (inset in Figure 3). An estimation gives 20 excitations per particle (no.$_{photons}$ per particle in the pump−probe volume of $\{500\ \mu m\}^3$) for the highest pump power and about 1 excitation at the lowest applied pump power. The linearity of the absorption intensity, in turn, means that the number of surface traps exceeds the number (20) of excited carriers.

One can further test if the observed transient absorption is indeed from populated trap states. The decay dynamics should be due to the detrapping process of the carriers. Therefore, the decay should be temperature dependent (thermal activation for escaping the trap potential) and should be largely independent for the number of populated trapping sites. To investigate this, we performed an excitation power variation and found that the decay time (2.55 ± 0.5 ns) of this transient absorption does not change, as shown in Figure 4, when excitation powers between 0.5 and 10 μJ/pulse, which translate to ~1−20 excitations per quantum dot, were applied.

The dip in the transient absorption spectrum around 510 nm (Figure 3) is found to be the superposition of transient absorption and transient bleach in this spectral range, as evidenced by the lowest energy transition occurring at 510 nm (Figure 1). Transient bleach occurs in quantum dots as a result of excited-state filling, which leads to a partial saturation of the band gap transition, as long as the excited states are populated. The combination of transient bleach and absorption should result in

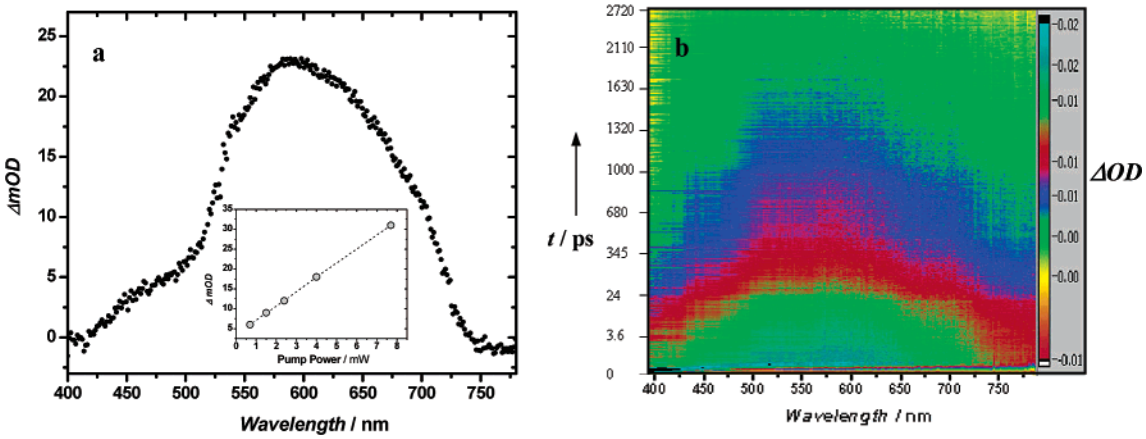

Figure 3. (a) Transient absorption spectra of $Cu_{1.8}S$ quantum dots after femtosecond laser excitation at 5 ps delay time. The inset shows the pump power dependence of the signal intensity. No saturation was observed up to 22 excitations per quantum dot. (b) Contour plot of the matrix of femtosecond transient absorption spectra (horizontal axis) versus time (vertical axis) reveals the global dynamics of the photoexcitation in the visible spectral range.

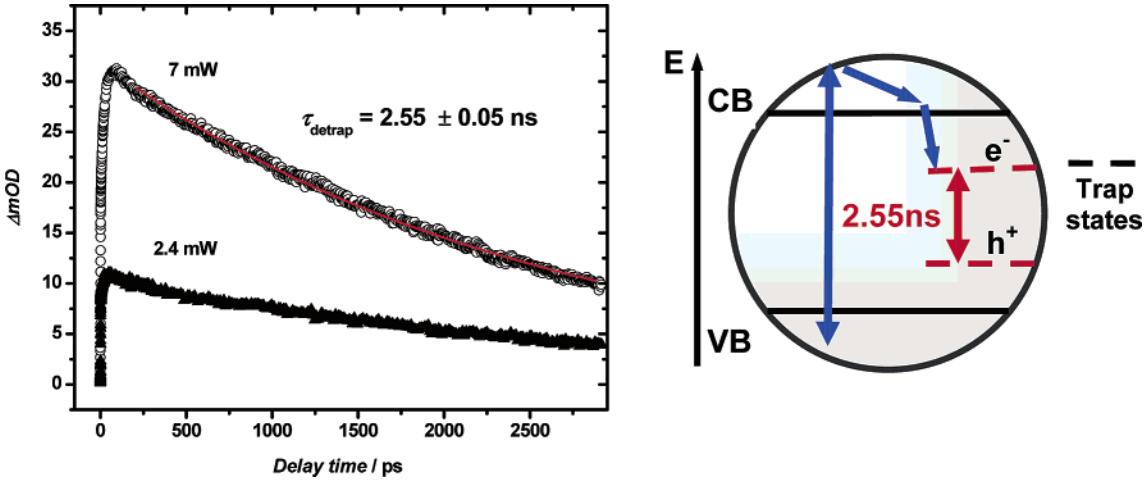

Figure 4. Nanosecond decay curve of the laser-induced transient absorption monitored at 600 nm, revealing the recombination time of the trapped electron and holes.

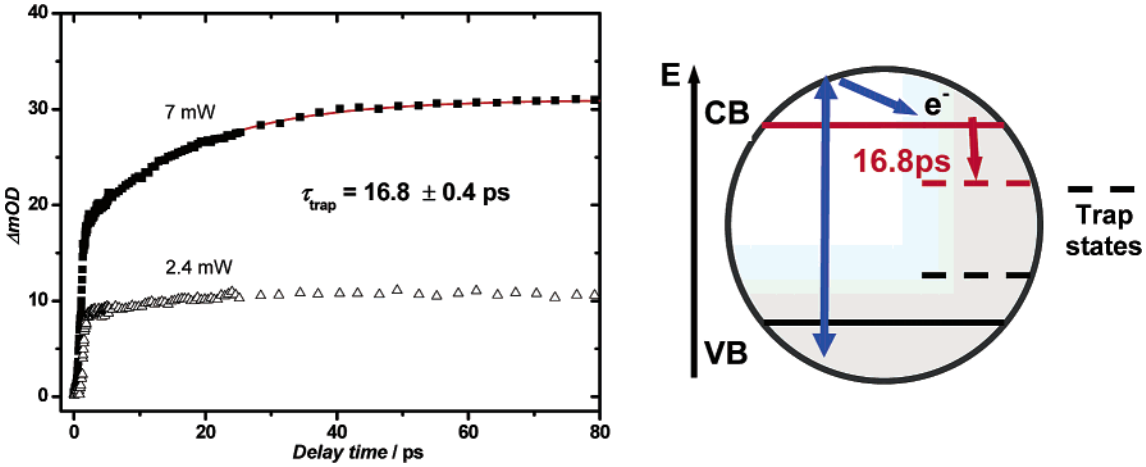

Figure 5. Picosecond rise time of the laser-induced transient absorption monitored at 600 nm, monitoring the conduction band depopulation and trapping of the photoexcited electron.

a more complex relaxation dynamics in the 500 nm range compared to the 600 nm (intraband gap) range, which is less than the band gap energy of the investigated quantum dot. Transient absorption in this energy range was previously assigned[31] to excited-state absorption originating from surface states, which occurs as a result of lattice defects and dangling bonds on the surface of the nanocrystals.

b. Trap-State Population and Depopulation. The lifetime of the transient absorption shown in Figure 4 was measured to be around 2.5 ns and reaches the time window of our experimental setup (3 ns), as shown in Figure 4. The relatively long lifetime indicates that the monitored transient absorption is due to trapped charge carriers.

If the monitored absorption in Figures 3 and 4 is due to trapped carriers, then it should be possible to observe the trapping process, provided that it is not faster than our experimental time resolution of 120 fs. Figure 5 shows the rise of the transient absorption in Figure 3, as monitored at 600 nm after excitation with a 120 fs laser pulse.

From the analysis of the rise of the transient absorption, a fast increase in absorption is observed within the first 400 fs. This increase is likely due to excited-state absorption of the delocalized hot carriers; however, fast carrier trapping on a subpicosecond time scale cannot be excluded.[31,35] In addition, a slower component (35%) with a rise time of 16.8 ps is observed, which can be assigned to the trapping process of carriers and the concomitant depopulation of the band edge. The slow-rising absorption becomes more prominent at high excitation powers, which underlines the interpretation of this transient as the trap-state population because at higher excitation densities the probability for electron trapping increases.

c. Electron Removal with Adsorbed Benzoquinone. As indicated above, it can be expected that intraband relaxation dynamics, i.e., population of the conduction band edge (via the bleach dynamics) and subsequent trapping (band edge depopulation, via trap-state absorption), can be observed in the range between 500 and 550 nm as bleaching of the ground-state absorption.

Using the technique of fast electron removal[36] via ultrafast electron transfer across the quantum dot interface, it is possible to assign the observed transients to the dynamics of either the electron or the hole. IR studies have shown that the carbonyl stretch vibration of the benzoquinone is lowered in frequency as soon as the benzoquinone adsorbs on the quantum dot surface.[37] The adsorbed benzoquinone acts then as an electron acceptor and removes the photoexcited electron from the conduction band in less time than the laser pulse duration (<120 fs). Therefore, the electron-transfer rate is faster than the experimental time resolution and as a result the pump−probe measurements in the presence of benzoquinone provide information about the remaining hole dynamics in the quantum dot. Thereby, detailed information about the dynamics of the electron or the hole can be obtained.[13,35,36,38,39]

Indeed, the kinetics monitored at 500 nm, shown in Figure 6 (black open cirlcles), is more complex than the one observed at 600 nm in Figure 7 (black open squares). This is due to the overlap of the ground-state bleaching with the broad trap-state absorption. It needs to be emphasized that the bleach is a negative transient signal as compared to the positive transient absorption. The measurement at 500 nm revealed a fast relaxation with 350 fs time component and a slower decay, which was fitted to a 2.2 ps exponential component. Furthermore, a 16 ps rise time is observed. Due to the opposite signs of bleach and transient absorption the dynamics has to be interpreted as follows: The 350 fs and 2.2 ps "decay" at 500 nm is actually the rise time of the bleach at the band edge due to the intraband relaxation of the electron and hole, respectively. The 16 ps "rise time" at 500 nm is actually the decay of the band edge bleach via trapping. The 16 ps component can be compared with the data obtained at 600 nm (Figure 5) and thereby be identified as the dynamics of the electron trapping process, because the trapping dynamics should be observable in both wavelength ranges via the formation of trap-state absorption.

Benzoquinone (BQ) was used as the electron acceptor on the quantum dot surface. Removal of the excited electron leads to the quenching of the transient features caused by transitions of the photoexcited electron. Hence, the 350 fs component, which was quenched by the electron acceptor, can be assigned to the intraband relaxation of the hot electron. On the other hand, the 2.2 ps component, which remains unquenched, is assigned to the relaxation of the hot hole. It is interesting to note that these relaxation times are quite similar to the times measured for the relaxation dynamics of the well-investigated CdS quantum dots.[36] This indicates similar effective masses and a quite similar density of states.

Also the 16 ps rise is quenched by BQ. It appears that with BQ on the surface no electrons can reach the trapping sites. Instead, a slower decay component of 39.7 ps is observed, which could be due to the trapping of the hole or the recombination of the carriers.

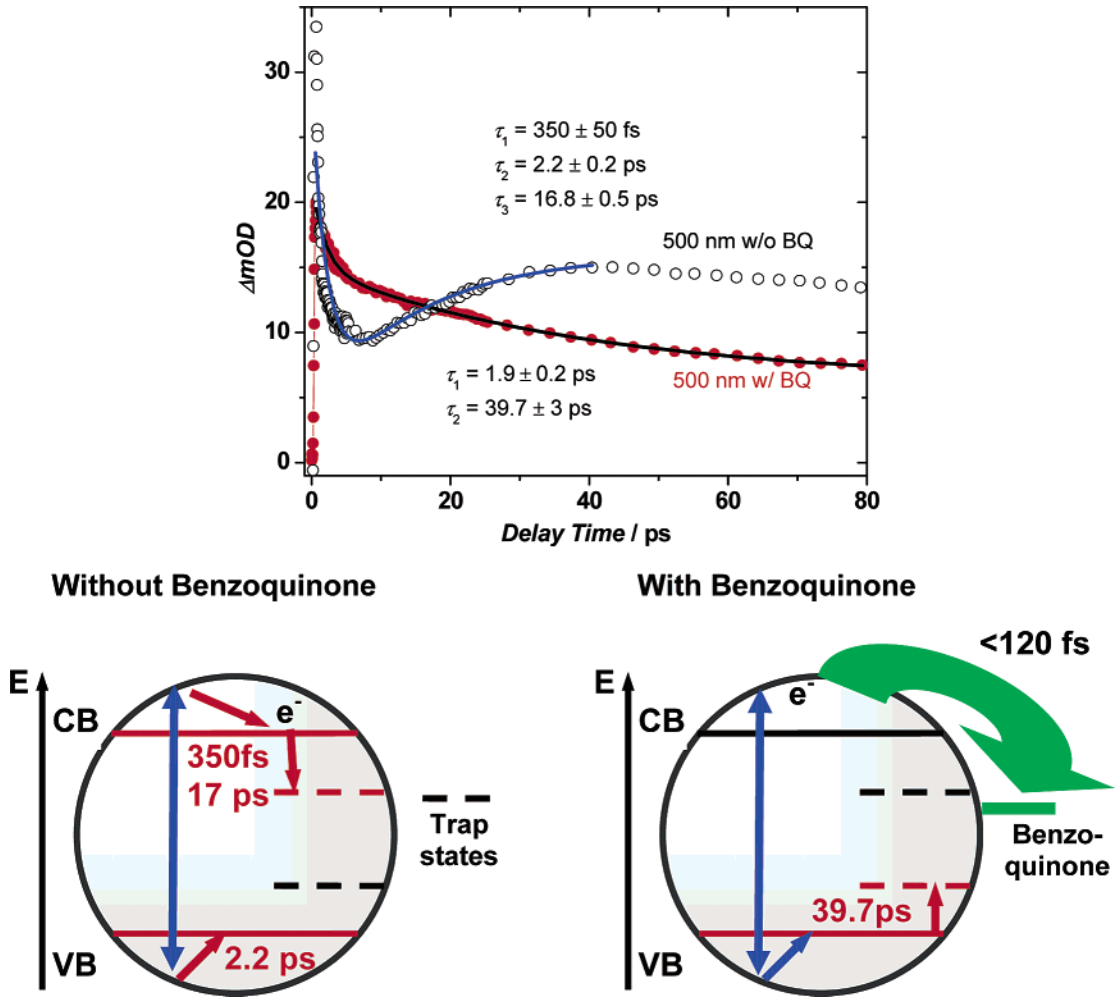

Figure 6. Relaxation dynamics of the transient absorption observed at 500 nm in a time window up to 80 ps. A fast decay (350 fs) and slower rise time (16.8 ps) are observed for the original sample without benzoquinone, indicating intraband relaxation and trapping of the photoexcited electrons. The 2.2 ps time component was identified as hole-cooling dynamics (see below).

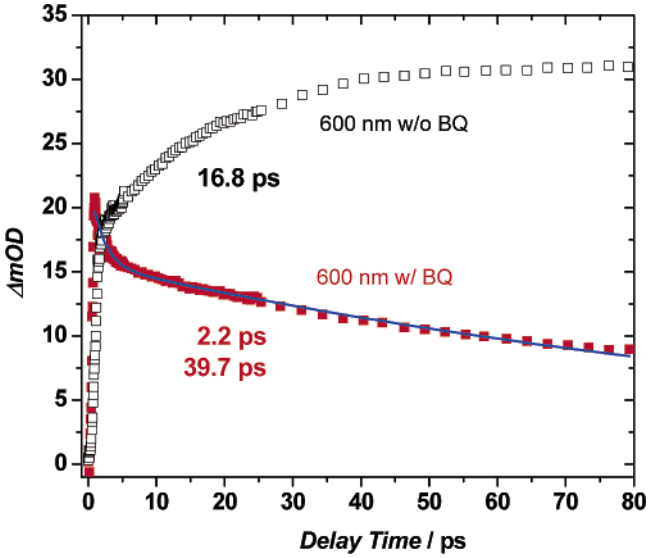

Figure 7. Relaxation dynamics of the transient absorption observed at 600 nm, measured up to 80 ps delay.

In comparison, the trap-state transients at 600 nm are simpler and easier to assign because the bleach dynamics are not overlapping at wavelengths >550 nm. The addition of BQ completely removed the 16 ps component shown in Figures 6 and 7 that was assigned to the trapping of electrons.

In addition, a new decay with a 2 ps component and a long lifetime component was recorded. The faster time component (2 ps) was mentioned before and can be assigned to the intraband relaxation of the hole. It has to be cautioned that this result is obtained in the presence of the benzoquinone on the quantum dot surface. However, these dynamics were monitored over a broad wavelength range (450−650 nm), giving good evidence that the method of electron removal utilized here is conclusive and reveals the dynamics due to the hole. The long lifetime component is therefore assigned to the recombination of the electron and the hole (in the presence of the electron acceptor on the surface).

d. Ground-State Recovery Versus Hole Trapping. Through the localization of the carriers during the trapping process, the overlap between electron and hole wave function can be drastically reduced, resulting in longer time components for the decay of the transient signals. Indeed, the decay of the transient absorption monitored at 600 nm, as presented in Figure 4, takes place on the 2.5 ns time scale. A similarly long lifetime component was also measured for the transient at 500 nm, as presented in Figure 8.

The addition of benzoquinone (BQ) reduced the lifetime of the recombination transient drastically from 2.5 ns to 471 ps. The decay of the transient absorption could be due to the depopulation of the hole trap states into deeper traps, according to a trap hopping mechanism. On the other hand, the recovery of the ground-state spectrum allows the conclusion of an

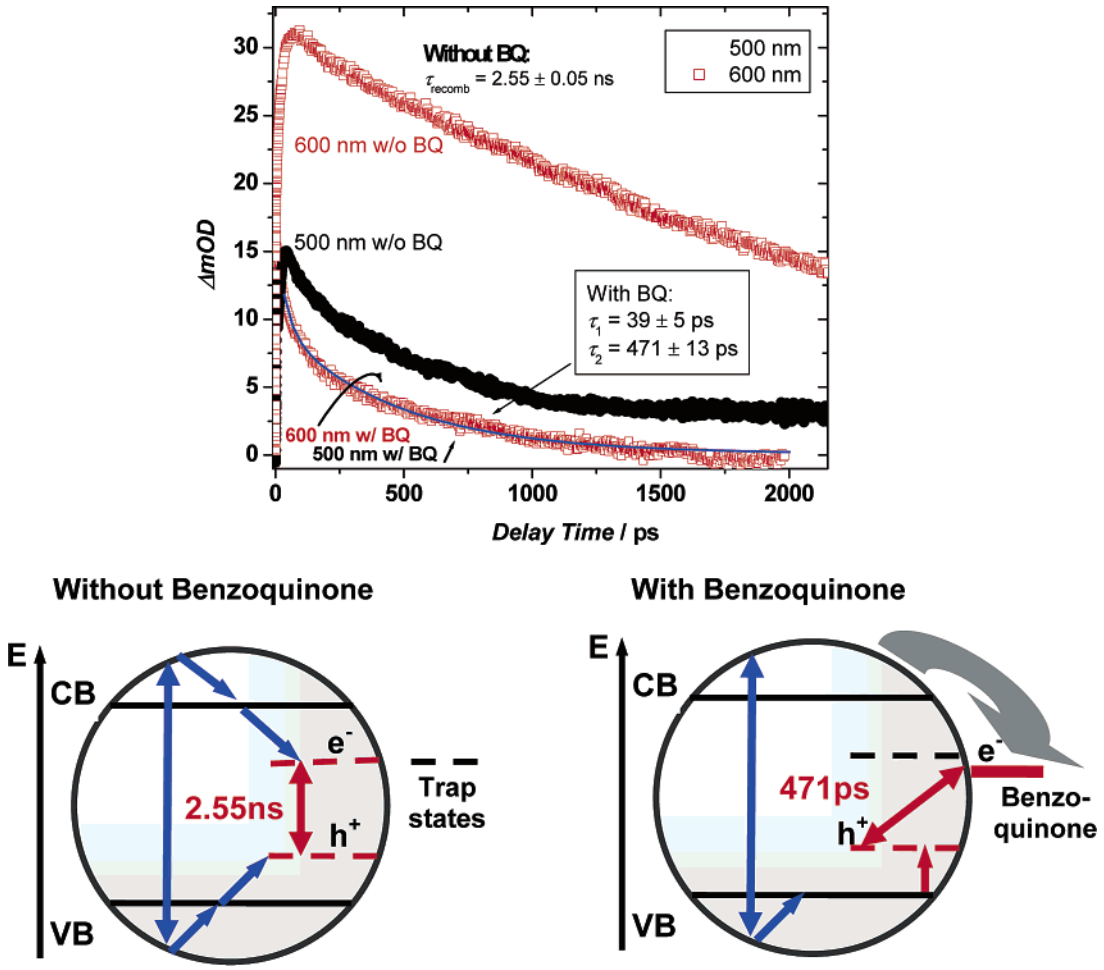

Figure 8. Decay dynamics of the transient absorption observed at 600 (red squares) and 500 nm (black circles) in a time window up to 2000 ps. Without benzoquinone the trap-state absorption displays a lifetime of several nanoseconds (≥2.5 ns). After adsorption of benzoquinone, the transient absorption is reduced in lifetime to <500 ps. This could be due to accelerated recombination of the electron with the hole due to trapping of the hole in the field of the BQ anion.

electron−hole recombination on the 471 ps time scale. One may conclude that, thereby, the recombination of the carriers is accelerated.

Conclusion

In summary, digenite ($Cu_{1.8}S$) quantum dot samples were prepared by simple pyrolysis of a precursor molecule $Cu(S_2CNEt_2)_2$ in the presence of TOPS. Electron and hole cooling, and their trapping dynamics, were investigated by femtosecond time-resolved pump−probe spectroscopy and selectively removing the photoexcited electron from the quantum dot via surface-adsorbed electron acceptors. Similar to CdS quantum dots, it is found for the digenite quantum dots that the electron relaxation is faster compared to the relaxation of the hole. The intraband relaxation times were measured to be 350 fs and 2.2 ps for the electron and hole, respectively. The trapping times were determined to be 17 and 40 ps for the electron and hole, respectively. The recombination time of the carriers in the photoexcited particle was found to be on the order of 2.5 ns. After the addition of benzoquinone to the quantum dot solution the electron−hole recombination time was reduced to less than 500 ps. In addition, the relaxation dynamics is strongly size dependent. Counterplaying effects make a prediction of an ideal size for long excited-state lifetimes difficult. Further experimental work on the size dependence of the optical properties is in progress.

Acknowledgment. We gratefully acknowledge the support through an NSF CAREER award (CHE-0239688) and the establishment of the Center for Chemical Dynamics and Nanomaterials Research through CWRU. We also are thankful for support through a NASA fellowship.

References and Notes

(1) Nirmal, M.; Brus, L. E. *Acc. Chem. Res.* **1999**, *32*, 407.
(2) Alivisatos, A. P. *Science* **1996**, *271*, 933.
(3) Colvin, V. L.; Schlamp, M. C.; Alivisatos, A. P. *Nature* **1994**, *370*, 354.
(4) Dabbousi, B. O.; Bawendi, M. G.; Onitsuka, O.; Rubner, M. F. *Appl. Phys. Lett.* **1995**, *66*, 1316.
(5) O'Regan, B.; Gratzel, M. *Nature* **1991**, *353*, 737.
(6) Kamat, P. V.; Meisel, D. E. *Semiconductor Nanoclusters − Physical, Chemical and Catalytic Aspects*; Elsevier: Amsterdam, 1997.
(7) Eychmuller, A.; Hasselbarth, A.; Katsikas, L.; Weller, H. *Ber. Bunsen-Ges. Phys. Chem.* **1991**, *95*, 79.
(8) Skinner, D. E.; Colombo, J. D. P.; Cavaleri, J. J.; Bowman, R. M. *J. Phys. Chem.* **1995**, *99*, 7853.
(9) Zhang, J. Z.; O'Neil, R. H.; Roberti, T. W. *J. Phys. Chem.* **1994**, *98*, 3859.
(10) Woggon, U.; Geissen, H.; Gindele, F.; Wind, O.; Fluegel, B.; Peyghambarian, N. *Phys. Rev. B* **1996**, *54*, 17681.
(11) Klimov, V. I.; McBranch, D. W. *Phys. Rev. Lett.* **1998**, *80*, 4028.
(12) Klimov, V. I.; Schwarz, C. J.; McBranch, D. W.; Leatherdale, C. A.; Bawendi, M. G. *Phys. Rev. B* **1999**, *60*, R2177.
(13) Klimov, V. I.; Milhailosky, A. A.; McBranch, D. W.; Leatherdale, C. A.; Bawendi, M. G. *Phys. Rev. B* **2000**, *61*, R13349.
(14) Guyot-Sionnest, P.; Shim, M.; Matranga, C.; Hines, M. *Phys. Rev. B* **1999**, *60*, R2181.

(15) Kim, S. H.; Wolters, R. H.; Heath, J. R. *J. Chem. Phys.* **1996**, *105*, 7957.
(16) Micic, O. I.; Cheong, H. M.; Fu, H.; Zunger, A.; Sprague, J. R.; Mascarenhas, A.; Nozik, A. J. *J. Phys. Chem. B* **1997**, *101*, 4904.
(17) Langof, L.; Ehrenfreund, E.; Lifshitz, E.; Micic, O. I.; Nozik, A. J. *J. Phys. Chem. B* **2002**, *106*, 1606.
(18) Cavaleri, J. J.; Colombo, J. D. P.; Bowman, R. M. *J. Phys. Chem. B* **1998**, *102*, 2, 1341.
(19) Nozik, A. J. *Annu. Rev. Phys. Chem.* **2001**, *52*, 193.
(20) Pankove, J. I. *Optical Processes in Semiconductors*; Dover: New York, 1975.
(21) Sze, S. *Physics of Semiconductor Devices*; Wiley: New York, 1981.
(22) Green, M. A. *Solar Cells*; University New South Wales: Kensington, Australia, 1992.
(23) Nozik, A. J. *Annu. Rev. Phys. Chem.* **1978**, *29*, 189.
(24) Huynh, W. U.; Ditter, J. J.; Alivisatos, A. P. *Science* **2002**, *295*, 2425.
(25) Huynh, W. U.; Peng, X.; Alivisatos, A. P. *Adv. Mater.* **1999**, *11*, 923.
(26) Reijnen, L.; Meester, B.; Goosens, A. *Mater. Sci. Eng. C* **2002**, *10*, 311.
(27) Dameron, C. T.; Reese, R. N.; Mehra, R. K.; Kortan, A. R.; Carroll, P. J.; Steigerwald, M. L.; Brus, L. E.; Winge, D. R. *Nature* **1989**, *338*, 596.
(28) Rogach, A. L.; Katsikas, L.; Kornowski, D. S. S.; Eychmuller, A.; Weller, H. *Ber. Bunsen-Ges.* **1996**, *100*, 1772.
(29) Bae, W.; Mehra, R. K. *J. Inorg. Biochem.* **1998**, *70*, 125.
(30) Torres-Martinez, C. L.; Nguyen, L.; Kho, R.; Bae, W.; Bozhilov, K.; Klimov, V. I.; Mehra, R. K. *Nanotechnology* **1999**, *10*, 340.
(31) Brelle, M. C.; Torres-Martinez, C. L.; McNulty, J. C.; Mehra, R. K.; Zhang, J. Z. *Pure Appl. Chem.* **2000**, *72*, 101.
(32) Lou, Y.; Samia, A. C. S.; Cowen, J.; Banger, K.; Chen, X.; Lee, H.; Burda, C. *Phys. Chem. Chem. Phys.* **2003**, *5*, 1091−5.
(33) Bonneau, R.; Wirz, J.; Zuberbuhler, A. D. *Pure Appl. Chem.* **1997**, *69*, 979.
(34) Klimov, V. I.; Karavanskii, V. A. *Phys. Rev. B* **1996**, *54*, 8087−94.
(35) Chikan, V.; Kelley, D. F. *Nano Lett.* **2002**, *2*, 1015−20.
(36) Burda, C.; Link, S.; Mohammed, M.; El-Sayed, M. *J. Phys. Chem. B* **2001**, *105*, 12286.
(37) Burda, C.; Green, T. C.; Link, S.; El-Sayed, M. *J. Phys. Chem. B* **1999**, *103*, 1783.
(38) Klimov, V. I.; Mikhailovsky, A. A.; McBranch, D. W.; Leatherdale, C. A.; Bawendi, M. G. *Phys. Rev. B* **2000**, *61*, R13349−52.
(39) Yu, D.; Wang, C.; Guyot-Sionnest, P. *Science* **2003**, *300*, 1277−80.